FUDMA Journal of Sciences (FJS)
ISSN online: 2616-1370
ISSN print: 2645 - 2944
Vol. 10 No. 10, May, 2026, pp 302 – 315
DOI: https://doi.org/10.33003/fjs-2026-1010-5498

Salicylaldimine Based Complexes and their Ascorbic Acid Ternary Analogues: Synthesis, Characterisation, Antimicrobial Evaluation, Molecular Docking and DFT Considerations

***[1]Raymond Akong Akong, [1]Desmond Chibuike Mmadu, [1,2]Samuel Kelechi Anyanwu, [3]Isiaka Mohammed and [1]Joseph Anthony Orighomisan Woods**

[1]Inorganic Chemistry Unit, Department of Chemistry, Faculty of Science, University of Ibadan, Ibadan, Oyo State, Nigeria.
[2]Department of Chemistry, Federal University of Technology Minna, Niger State, Nigeria.
[3]Organic Chemistry Unit, Department of Chemistry, Faculty of Science, University of Ibadan, Ibadan, Oyo State, Nigeria.

*Corresponding authors' email: ramondak@yahoo.com

ABSTRACT

This study reports a series of complexes with the general formula $[M(A_1)_2(H_2O)_2]\cdot nH_2O$ (1 – 4) and $[M(A_1)(A_2)(H_2O)_2]\cdot nH_2O$ (5 – 8) {where M = Co, Ni, Cu and Zn; HA_1 = (*E*)-2-(hydrazineylidenemethyl)phenol and HA_2 = ascorbic acid}. The prepared compounds were characterised by ^{1}H nmr, Fourier Transform infrared (FTIR) and electronic spectroscopies as well as magnetic susceptibility measurement. Quantum calculation were carried out using DFT/B3LYP-D3/6-31G** for the ligands and DFT/B3LYP-D3/LACVP** for the complexes. The magnetic moments for the Co(II) {5.06 – 5.49 B.M} and Ni(II) {3.15 – 3.16 B.M} complexes suggest octahedral geometry, with orbital contribution. The Cu(II) complexes appear to be octahedral with the homoleptic complex (3) displaying a subnormal value (1.58 B.M). Generally, the complexes showed better antimicrobial activity than the ligands. The mixed ligand complexes showed better activity than respective homoleptic analogue – while the mixed ligand complexes displayed Minimum Inhibitory Concentration (MIC) in the range 0.125 – 2.00 mg/mL, the homoleptic complexes displayed MIC in range 0.50 – 2.00 mg/mL. The Ni(II) mixed ligand complex, 6, recorded the highest (negative) docking scores; -5.667 kcal/mol, -6.614 kcal/mol and -5.542 kcal/mol against *E. coli*, *S. aur* and *C. alb*, respectively – with better scores than ciprofloxacin (-5.379 kcal/mol and -4.183 kcal/mol against *E. coli* and *S. aur*, respectively) but lower than ketoconazole (-8.288 kcal/mol against *C. alb*); 6 also displayed the best global softness (0.6196 eV^{-1}), in comparison to other complexes (except for the spin down {β} variants of compounds 3 and 7 {3_β and 7_β}). Thus, the prepared compounds are potential antimicrobial agents.

Keywords: Salicylaldehyde, Schiff Bases, Binary/Mixed-Ligand Complexes, Biological Evaluation, DFT Calculation

INTRODUCTION

The hydrazide-hydrazone subclass of Schiff bases (imines) as well as their metal complexes are known to be useful in different areas of medicine and have been deployed as antimicrobial, antitumour, antimalarial, anti-inflammatory, anti-oxidizing, antituberculosis agents (Rupa *et al.*, 2022; Ribeiro and Correia 2024; Tafere *et al.*, 2025; Rathi *et al.*, 2026; El-Sherbini *et al.*, 2026; Ieque *et al.*, 2024). The salicylaldehyde core is a prominent feature in many hydrazide-hydrazones with biological potential (Abdelrhman *et al.*, 2021; Demirbağ *et al.*, 2025; El-Sherif *et al* 2012) – the propensity for chelate formation being a major drive.

Ascorbic acid (Vitamin C) is an essential micronutrient (for humans) and the application of ascorbic acid, its derivatives and metal complexes in biology has been a subject of many research efforts (Gęgotek and Skrzydlewska 2022; Wadday and Hussein 2022; Lu *et al.*, 2007; Kaushik *et al.*, 2025).

The increasing incidence of antibiotic/antimicrobial drug resistance accounts for a large number of death globally (Antimicrobial Resistance Collaborators 2022; Duffey *et al.*, 2024), thus there is a great need for the design and preparation of materials with potentials to tackle the challenge of drug resistance. Although mixed ligand complexes of ascorbic acid are known in literature (Yuge and Miyamoto 2002; Yuge and Miyamoto 1996; Hollis *et al.*, 1987; Malviy *et al.*, 2021; Onyenze *et al.*, 2016), biological evaluation has been reported for only a few (Malviy *et al.*, 2021; Onyenze *et al.*, 2016). In this study, we report four (4) salicylaldimine hydrazide-hydrazone based binary complexes as well as their respective ternary complex with ascorbic acid {Scheme 1}. The biological evaluation of the compounds (against *Staphylococcus aureus*, *Bacillus subtilis*, *Escherichia coli*, *Pseudomonas aeruginosa*, *Candida albicans* and *Trichophyton rubrum*) as well as their molecular docking (against *Escherichia coli*, *Staphylococcus aureus* and *Candida albicans* proteins) is herein reported.

Preparation of Hydrazide-Hydrazone, HA_1, and its Homoleptic and Heteroleptic Complexes

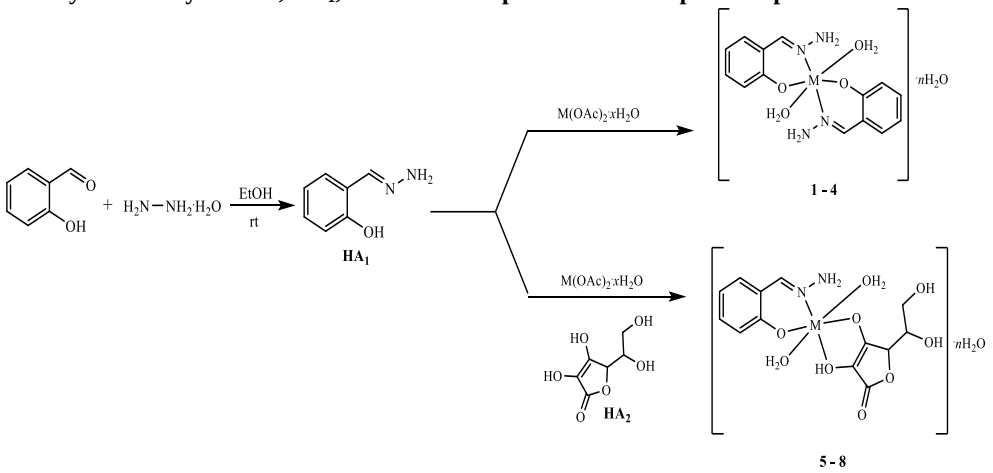

MATERIALS AND METHODS

General Information

All starting materials for synthesis were obtained commercially as reagent grade and used as supplied. Infrared (IR) spectral data were collected on a PerkinElmer spectrometer in the range 4000 – 400 cm^{-1}. UV-Vis spectra were recorded on a Spectroquant Pharo 300 Spectrophotometer. ^1H NMR spectra was recorded with a Nanalysis pro 60 NMReady table top spectrometer. A Stuart Melting Point (SMP10) apparatus was used for melting point determination. Ethylene Diamine Tetraacetic Acid (EDTA) titrimetry was used for percentage metal determination. Magnetic measurements were carried out using a Sherwood Magnetic Susceptibility Balance. Density functional theory (DFT) calculations were carried out using the Maestro Schrödinger programme (Jaguar, version 11.9) with B3LYP-D3 method and 6-31G** and LACVP** basis sets used for the ligands (**HA_1** and **HA_2**) and metal complexes (**1** – **8**), respectively; while molecular docking was done with the extra precision (XP) mode of the Glide function of Maestro Schrödinger – with the selected protein receptors obtained from the protein data bank (PDB) website: Outer membrane Protein A (OMPA) Transmembrane domain of *Escherichia coli* (PDB ID: 1BXW, 2.50 Å) (Pautsch and Schulz 1998) *Staphylococcus aureus* (PDB ID: 6SNR, 1.62 Å) (York *et al*., 2021) and *Candida albicans* protein geranylgeranyltransferase-I complexed with GGPP (PBD ID: 3DRA, 1.80 Å) (Hast and Beese 2008).

Antimicrobial Susceptibility Testing (AST)

20 mL sterilised Mueller Hinton Agar (Oxoid) was aseptically dispensed into sterile petri dishes. The agar was allowed to set for about 10 minutes after which the petri dishes, containing the agar, were dried in a hot air oven to remove moisture from the cover of the plate as well as the surface of the agar. Using the spread plate method, 10^{-5} diluted of an 18-hour broth adjusted to McFarlan standard, was spread on the surface of the agar using sterile cotton swab. After this, a 6 mm cork borer was flamed, allowed to cool and used to bore wells into the inoculated agar. The already prepared samples (of different concentrations) were added to the bored wells and labelled appropriately. The positive control, ciprofloxacin (for bacteria)/ ketoconazole (for fungi), was placed in one of the bored wells. The solvent dimethyl sulphoxide (DMSO) was used as a negative control to ensure it has no activity against the organisms. The plates were left for about an hour to allow for proper diffusion of the samples and then incubated at 37°C for 24 hours. The diameter of zones of inhibition were measured in mm. Two (2) Gram positive (*Staphylococcus aureus* and *Bacillus subtilis*); two (2) Gram negative (*Escherichia coli* and *Pseudomonas aeruginosa*) as well as two (2) fungi (*Candida albicans* and *Trichophyton rubrum*) were used.

Determination of Minimum Inhibitory Concentration (MIC)

The MIC was done using broth micro dilution method and 96 well plates were used. The samples were dissolved in double strength Tryptone Soya Broth (Merck) to obtain a solution of 2.5 mg/mL. This was then diluted serially in sterile 96 well plate to obtain concentration in the range 0.01953125 – 1.25 mg/mL. Ciprofloxacin (10 µg/mL) and ketoconazole (10 µg/mL) were used as reference drugs for the anti-bacterial and anti-fungi assay, respectively. These drugs were also diluted to obtain concentrations in the range 0.1325 – 10.0000 µg/mL for the assay. After checking for growth or turbidity in the test plates (MIC determination), 10 µL of 0.2 mg/mL of *p*-iodonitrotetrazolium violet (*p*-INT) was added to the wells. The plates were further incubated at 37°C for 30 minutes. Wells with colour change from yellow to pinkish red indicated microbial growth.

Determination of Minimum Microbicidal Concentration (MMC)

Each of the micro plate wells were inoculated with 10 µL of the micro-organism and incubated at 37°C for 24 hours. The least concentrations which showed no growth or turbidity after hours of incubations were streaked on nutrient agar. The least concentrate which showed no trace of growth was taken as the MMC.

Preparation of (E)-2-(hydrazineylidenemethyl)phenol (HA_1)

The Schiff base HA_1 was prepared via a previous procedure (Okafor 1978). 10 mL ethanol solution of 3 mL (3.438 g, 0.0282 mol) of salicylaldehyde was added in portions to a 7 mL ethanol solution of 1.4 mL (1.4448 g, 0.0289 mol) hydrazine monohydrate, at room temperature. The precipitate obtained upon complete addition of salicylaldehyde was stirred for about 30 minutes, filtered washed with ethanol and dried under vacuum to afford an off-white product. Yield (2.7355 g, 71.37 %) m.p 218 °C; ^1H NMR (60 MHz, DMSO-d_6) δ (ppm) 8.11 (s, 1H, CH=N), 6.80 (d, *J* = 7.0 Hz, 1H, Ar-H), 6.48 (d, *J* = 7.5 Hz, 1H, Ar-H), 6.12 (d, *J* = 5.2 Hz, 1H,

Ar-H). Selected IR (ATR, cm^{-1}): 1615s, 1570s, 1479s, 1271s, 1195s, 1030s, 969s, 894s, 728s, 568s, 466s, 420s. UV-Vis (DMSO, nm {ε /M^{-1} cm^{-1}}): 299 {21,090}, 360 {22,240}.
Ascorbic acid (HA_2): Selected IR (ATR, cm^{-1}): 3525s, 3404s, 3313w, 1752s, 1650s, 1317s, 1197w, 1023s, 986s, 868s, 820s, 628s, 564s, 447s. UV-Vis (DMSO, nm {ε /M^{-1} cm^{-1}}): 299 {13,360}, 351 {7,600}sh.

Preparation of Homo- and Heteroleptic Complexes

The homoleptic complexes (1 – 4) were prepared by reacting appropriate metal acetate salt with HA_1 in 1:2 ratio; while the heteroleptic complexes (5 – 8) were prepared by reacting equimolar amounts of metal acetate salt, HA_1 and ascorbic acid (HA_2). The addition of triethyl amine (TEA) was required for precipitation of the heteroleptic zinc complex. The precipitates obtained were washed with EtOH and dried under vacuum

$[Co(A_1)_2(H_2O)_2]2H_2O$ (1), orange: 0.1841 g (0.00074 mol) of $Co(OAc)_2{\cdot}4H_2O$ was dissolved in 10 mL of EtOH. 10 mL EtOH slurry of HA_1 (0.2010 g, 0.00148 mol) was added, and the resulting orange mixture heated to reflux, with constant stirring for 4 hours. The precipitate obtained was filtered, washed and dried. Yield (0.2004 g, 67.7 %) m.p > 300°C. Selected IR (ATR, cm^{-1}): 1615s, 1602s, 1541s, 1470s, 1446s, 1283s, 1152s, 966s, 862s, 756s, 584s, 451s. UV-Vis (DMSO, nm {ε /M^{-1} cm^{-1}}): 288 {12,620}, 388 {12,690}. %Metal Theor. (Exp.) = 14.69 % (14.73 %). μ_{eff} = 5.49 BM

$[Ni(A_1)_2(H_2O)_2]$ (2), lemon: 0.1877 g (0.00075 mol) of $Ni(OAc)_2{\cdot}4H_2O$ was dissolved in 10 mL of EtOH. 10 mL EtOH slurry of HA_1 (0.2020 g, 0.00148 mol) was added, and the resulting lemon mixture heated to reflux, with constant stirring for 4 hours. The precipitate obtained was filtered, washed and dried. Yield (0.2148 g, 79.3 %) m.p > 300°C. Selected IR (ATR, cm^{-1}): 1615s, 1603s, 1540s, 1469s, 1448s, 1290s, 1190s, 1150s, 962s, 898s, 755s, 584s, 453s. UV-Vis (DMSO, nm {ε /M^{-1} cm^{-1}}): 289 {9,520}, 401 {9,570}. %Metal Theor. (Exp.) = 16.08 % (16.21 %). μ_{eff} = 3.15 BM

$[Cu(A_1)_2(H_2O)_2]$ (3), brownish yellow: 0.0736 g (0.00037 mol) of $Cu(OAc)_2{\cdot}H_2O$ was dissolved in 10 mL of EtOH. 10 mL EtOH slurry of HA_1 (0.1001 g, 0.00074 mol) was added, and the resulting brownish-yellow mixture heated to reflux, with constant stirring for 4 hours. The precipitate obtained was filtered, washed and dried. Yield (0.0607 g, 44.6 %) m.p > 300°C. Selected IR (ATR, cm^{-1}): 1602s, 1586s, 1450s, 1325s, 1195s, 1148s, 1130s, 968s, 751s, 594s, 459s. UV-Vis (DMSO, nm {ε /M^{-1} cm^{-1}}): 297 {16,940}, 359 {13,030}, 410 {7,650}sh. %Metal Theor. (Exp.) = 17.18 % (17.16 %). μ_{eff} = 1.58 BM

$[Zn(A_1)_2(H_2O)_2]7H_2O$ (4), yellow: 0.1617 g (0.00074 mol) of $Zn(OAc)_2{\cdot}2H_2O$ was dissolved in 10 mL of EtOH. 10 mL EtOH slurry of HA_1 (0.2003 g, 0.00147 mol) was added, and the resulting yellow mixture heated to reflux, with constant stirring for 4 hours. The precipitate obtained was filtered, washed and dried. Yield (0.1807 g, 49.3 %) m.p > 300°C. Selected IR (ATR, cm^{-1}): 3363w, 1619s, 1489s, 1386s, 1276s, 1195s, 893s, 749s, 565s, 422s. UV-Vis (DMSO, nm {ε /M^{-1} cm^{-1}}): 299 {16,270}, 360 {12,280}, 409 {7,810}sh. %Metal Theor. (Exp.) = 13.13 % (13.12 %). μ_{eff} = Diamagnetic

$[Co(A_1)(A_2)(H_2O)_2]2.25H_2O$ (5), light brown: 0.5478 g (0.0022 mol) of $Co(OAc)_2{\cdot}4H_2O$ was dissolved in 10 mL of EtOH. 6 mL EtOH slurry of HA_1 (0.3004 g, 0.0022 mol) and 5 mL EtOH solution of HA_2 (0.3876 g, 0.0022 mol) were added simultaneously, and the resulting orange solution heated to reflux, with constant stirring for 4 hours. The precipitate obtained was filtered, washed and dried. Yield (0.4288 g, 43.6 %) m.p > 300°C. Selected IR (ATR, cm^{-1}): 3368br, 1616s, 1486w, 1358s, 1316s, 1274s, 1197w, 893s, 749s, 550w, 458s. UV-Vis (DMSO, nm {ε /M^{-1} cm^{-1}}): 296 {25,300}, 361 {25,690}. %Metal Theor. (Exp.) = 13.22 % (13.21 %). μ_{eff} = 5.06 BM

$[Ni(A_1)(A_2)(H_2O)_2]2.25H_2O$ (6), yellow: 0.5475 g (0.0022 mol) of $Ni(OAc)_2{\cdot}4H_2O$ was dissolved in 10 mL of EtOH. 6 mL EtOH slurry of HA_1 (0.3003 g, 0.0022 mol) and 5 mL EtOH solution of HA_2 (0.3884 g, 0.0022 mol) were added simultaneously, and the resulting lemon solution heated to reflux, with constant stirring for 4 hours. The precipitate obtained was filtered, washed and dried. Yield (0.3809 g, 38.8 %) m.p > 300°C. Selected IR (ATR, cm^{-1}): 3360br, 1616s, 1540w, 1471s, 1361w, 1317w, 745w, 455w, 422w. UV-Vis (DMSO, nm {ε /M^{-1} cm^{-1}}): 297 {25,500}, 360 {25,960}. %Metal Theor. (Exp.) = 13.17 % (13.14 %). μ_{eff} = 3.16 BM

$[Cu(A_1)(A_2)(H_2O)_2]0.50H_2O$ (7), brown: 0.4391 g (0.0022 mol) of $Cu(OAc)_2{\cdot}H_2O$ was dissolved in 10 mL of EtOH. 6 mL EtOH slurry of HA_1 (0.3001 g, 0.0022 mol) and 5 mL EtOH solution of HA_2 (0.3874 g, 0.0022 mol) were added simultaneously, and the resulting light brown solution heated to reflux, with constant stirring for 4 hours. The precipitate obtained was filtered, washed and dried. Yield (0.4411 g, 47.8 %) m.p > 300°C. Selected IR (ATR, cm^{-1}): 3320br, 1600s, 1533s, 1467s, 1314s, 1195s, 1149s, 753s, 591s, 459s. UV-Vis (DMSO, nm {ε /M^{-1} cm^{-1}}): 298 {5,760}, 356 {4,900}. %Metal Theor. (Exp.) = 15.17 % (15.23 %). μ_{eff} = 1.91 BM

$[Zn(A_1)(A_2)(H_2O)_2]8H_2O$ (8), yellow: 0.4828 g (0.0022 mol) of $Zn(OAc)_2{\cdot}2H_2O$ was dissolved in 10 mL of EtOH. 6 mL EtOH slurry of HA_1 (0.3003 g, 0.0022 mol) and 5 mL EtOH solution of HA_2 (0.3878 g, 0.0022 mol) were added simultaneously, and the resulting yellow solution heated to reflux, with constant stirring. Drops of triethyl amine (TEA) was added after 2 hours and the reaction was continued for another 2 hours. The precipitate obtained was filtered, washed and dried. Yield (0.3559 g, 29.0 %) m.p > 300°C. Selected IR (ATR, cm^{-1}): 1619s, 1572w, 1486s, 1383s, 1277s, 1197s, 784s, 750s, 565w, 458s. UV-Vis (DMSO, nm {ε /M^{-1} cm^{-1}}): 298 {19,340}, 359 {20,480}. %Metal Theor. (Exp.) = 11.76 % (17.71 %). μ_{eff} = Diamagnetic

RESULTS AND DISCUSSION

Synthesis, Electronic/Infrared Spectroscopy and Magnetic Properties of the Compounds

The imine HA_1 and complexes 1 and 2 were obtained in relatively good yields (67 – 79 %), while all other complexes (3 – 8) were obtained in relatively low yields (29 – 49 %). The ^{1}H nmr of HA_1 (Fig. 1) bears some semblance to a previous report (Gupta *et al*., 2017), with the imine (CH=N) proton appearing at 8.71 ppm but the aromatic protons were observed around 6 – 7 ppm. In the electronic measurements of the compounds, the imine HA_1 exhibited peaks at 299 nm and 360 nm (Fig. 2{a}) ascribed to $\pi \rightarrow \pi^*$ and $n \rightarrow \pi^*$ transitions, respectively. In the homoleptic complexes a blue shift is observed for the $\pi \rightarrow \pi^*$ peak, alongside charge transfer (CT) transitions (Fig. 2{a}). In the mixed ligand complexes (Fig. 2{b}) the blue shift in $\pi \rightarrow \pi^*$ peak is not observed but a slight red shift (5 – 10 nm) in the $n \rightarrow \pi^*$ peak is observed. The Infrared (IR) spectra of the compounds (Fig. 3) revealed the imine (C=N) band of HA_1 at 1615 cm^{-1} (Fig. 3{a}) which shifts to 1602 – 1603 cm^{-1} for complexes 1 – 3 and 1619 cm^{-1} for 4 (Fig. 3{b}). The ascorbic acid HA_2 displayed its -OH band around 3404 – 3525 cm^{-1} (Fig. 3{a}), which shifts, in the mixed ligand complexes, to 3320 – 3368 cm^{-1} – the imine bands in the mixed ligand complexes also appear at 1600 – 1619 cm^{-1} (Fig. 3{c}).

The observed magnetic moment of the cobalt complexes 1 (5.49 B.M) and 5 (5.06 B.M) are higher than expected for d^7 ($e^4t_2^3$) tetrahedral complexes (4.3 – 4.7 B.M), but are close to

the expected range for high spin d^7 ($t_{2g}^5 e_g^2$) octahedral complexes (4.7 – 5.2 B.M). The values are higher than expected spin only (μ_s) value for three unpaired electrons (3.87 B.M) suggesting significant orbital contribution from the $^4T_{1g}$ ground state (Jha and Ray 2000; El-Gammal *et al*., 2021; Dey *et al*., 2025). The observed magnetic moment of the nickel complexes 2 (3.15 B.M) and 6 (3.16 B.M) are lower than expected for d^8 ($e^4 t_2^4$) tetrahedral complexes (3.5 – 4.2 B.M), but in the range expected for d^8 ($t_{2g}^6 e_g^2$) octahedral complexes (2.9 – 3.4 B.M). The values are slightly higher than expected spin only (μ_s) value for two unpaired electrons (2.83 B.M) suggesting orbital contribution from the $^3A_{2g}$ ground state is not completely quenched (Jha and Ray 2000; El-Gammal *et al*., 2021). The homoleptic copper complex, 3, displayed a subnormal magnetic moment of 1.58 B.M, while the magnetic moment of the heteroleptic analogue, 7 (1.91 B.M), is in expected range for d^9 ($t_{2g}^6 e_g^3$) octahedral complexes (1.75 – 2.20 B.M) (Fabretti *et al*., 1982) – suggesting copper-copper/superexchange interaction(s) or antiferromagnetism in 3 (Fabretti *et al*., 1982; El-Asmy and Al-Hazmi 2009; Sogukomerogullari *et al*., 2025).

The spectroscopic and magnetic properties support the formulation of the complexes (Fig. 4).

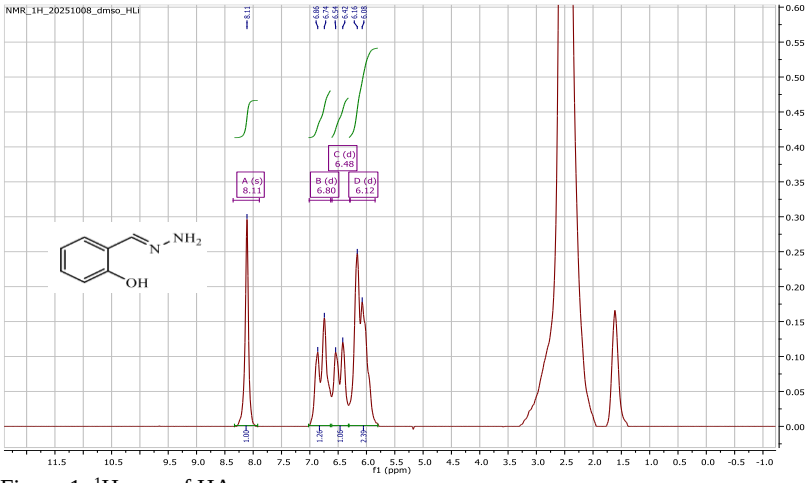

Figure 1: ^{1}H-nmr of HA_1

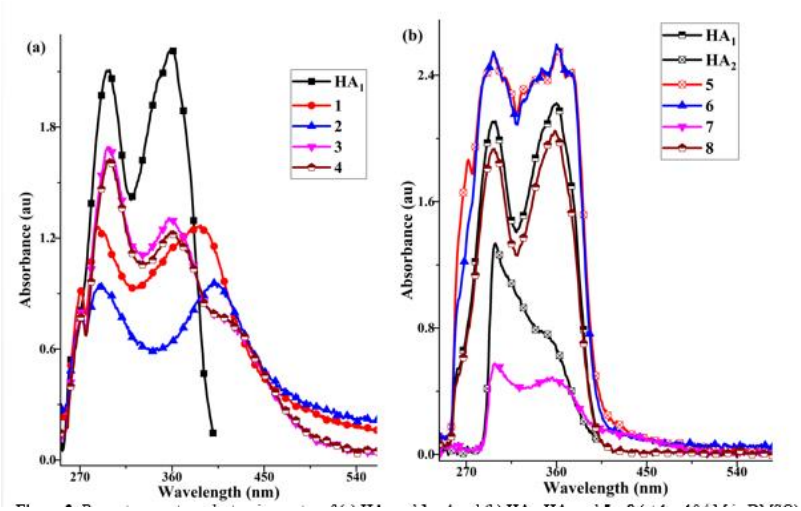

Figure 2: Room Temperature Electronic Spectra of (a) HA_1 and 1 – 4 and (b) HA_1, HA_2 and 5 – 8 (at 1×10^{-4} M in DMSO)

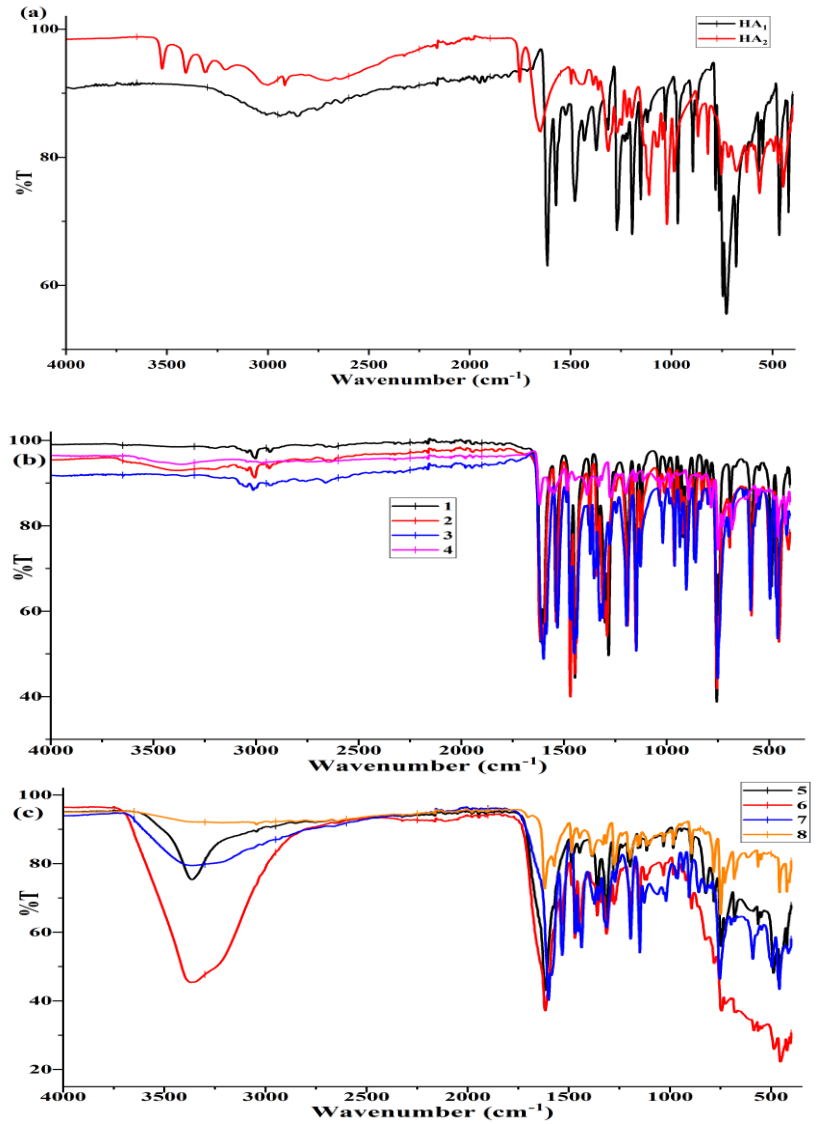

Figure 3: Infrared Spectra of (a) the ligands (b) homoleptic and (c) mixed ligand complexes

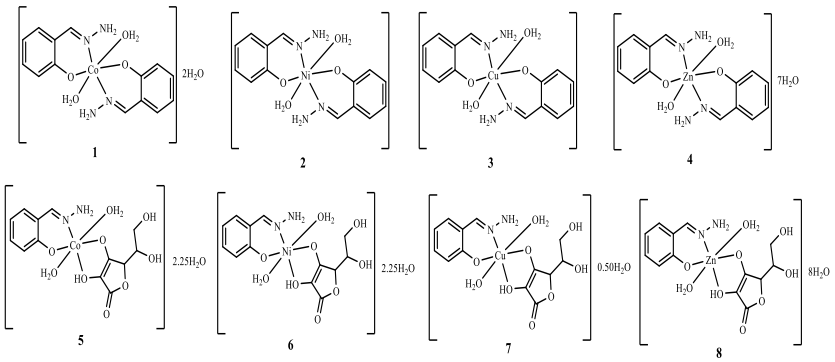

Figure 4: Proposed Structures for the Prepared Complexes

Biological Activity of the Compounds

The antimicrobial activity of the Schiff base (HA_1), co-ligand (HA_2) and the metal complexes (1 – 8) were tested against four bacteria and two fungi species using agar plate disc diffusion method at concentrations of 1.0 mg/mL and 2.0 mg/mL (Table 1). The homoleptic cobalt complex, 1, showed activity only against the Gram (+) bacteria species; all the other homoleptic complexes are active against the tested organisms except for 2, which is not active against *C. alb*. The heteroleptic complexes (5 – 8) generally displayed slightly better activity than corresponding homoleptic complex, and displayed higher activity than the standard, ciprofloxacin, against *B. sub*, *E. coli* and *P. aer*. Compound 6, however, did not display activity against *T. rub*.

The compounds displayed minimum inhibitory concentration (MIC) in the range 0.125 to > 2.00 mg/mL (Table 2) – the inactivity observed in compound 1, from the Antimicrobial Susceptibility Testing (AST) is still seen in its MIC data.

Generally, the compounds showed broad spectrum activity against tested organisms.

Table 1: Antimicrobial Susceptibility Testing (AST) for HA_1, HA_2 and 1 – 8 {Zones of growth inhibition (mm)}

		Gram Positive		***Gram Negative***		***Fungi***	
		S. aur	***B. sub***	***E. coli***	***P. aer***	***C. alb***	***T. rub***
Compounds	Conc. (mg/mL)						
HA_1	1.0	10	8	10	R	R	12
	2.0	14	14	15	10	12	14
HA_2	1.0	10	8	R	R	R	R
	2.0	12	12	R	10	10	R
1	1.0	R	8	R	R	R	R
	2.0	12	13	R	R	R	R
2	1.0	R	12	8	R	R	R
	2.0	10	15	14	10	R	12
3	1.0	8	8	R	13	R	10
	2.0	14	14	10	18	15	12
4	1.0	10	8	10	8	8	R
	2.0	12	15	15	15	12	10
5	1.0	10	14	R	14	14	8
	2.0	14	20	14	16	20	15
6	1.0	8	14	12	12	14	R
	2.0	12	18	18	14	16	R
7	1.0	12	14	14	14	R	12
	2.0	14	20	16	18	12	16
8	1.0	14	16	15	14	13	16
	2.0	18	18	18	20	18	18
Cipro		18	12	16	14	ND	ND
Ket		ND	ND	ND	ND	20	22
DMSO		No Activity					

Zones of growth inhibition are in millimeters (mm); R = Resistant to the sample; ND = Not determined; Conc. = Concentration; *S. aur = Staphylococcus aureus*; *B. sub = Bacillus subtilis*; *E. coli = Escherichia coli*; *P. aer = Pseudomonas aeruginosa*; *C. alb = Candida albicans*; *T. rub = Trichophyton rubrum*; *Cipro = Ciprofloxacin*; *Ket = Ketoconazole*

Table 2: Minimum Inhibitory Concentration (MIC) and Minimum Microbicidal Concentration (MMC) for HA_1, HA_2 and 1 – 8

	Gram Positive		***Gram Negative***		***Fungi***	
	S. aur	***B. sub***	***E. coli***	***P. aer***	***C. alb***	***T. rub***
Compounds						
HA_{1MIC}	0.50	1.00	2.00	> 2.00	> 2.00	1.00
HA_{1MMC}	1.00	1.00	> 2.00	> 2.00	> 2.00	2.00
HA_{2MIC}	1.00	1.00	> 2.00	> 2.00	> 2.00	> 2.00
HA_{2MMC}	2.00	> 2.00	> 2.00	> 2.00	> 2.00	> 2.00
1_{MIC}	> 2.00	2.00	> 2.00	> 2.00	> 2.00	> 2.00
1_{MMC}	> 2.00	> 2.00	> 2.00	> 2.00	> 2.00	> 2.00
2_{MIC}	> 2.00	2.00	2.00	> 2.00	> 2.00	> 2.00
2_{MMC}	> 2.00	> 2.00	> 2.00	> 2.00	> 2.00	> 2.00
3_{MIC}	0.50	1.00	> 2.00	0.50	2.00	> 2.00
3_{MMC}	1.00	2.00	> 2.00	2.00	2.00	> 2.00
4_{MIC}	0.50	0.50	2.00	2.00	2.00	> 2.00
4_{MMC}	2.00	0.50	2.00	> 2.00	2.00	> 2.00
5_{MIC}	2.00	0.50	2.00	1.00	0.25	0.50
5_{MMC}	2.00	2.00	2.00	2.00	0.50	0.50
6_{MIC}	0.50	0.125	0.25	> 2.00	0.50	> 2.00
6_{MMC}	1.00	0.50	0.25	> 2.00	0.50	> 2.00
7_{MIC}	0.125	0.50	0.50	0.50	2.00	0.50
7_{MMC}	1.00	1.00	0.50	2.00	> 2.00	0.50
8_{MIC}	0.25	0.25	0.50	1.25	0.25	0.25
8_{MIC}	0.50	0.25	0.50	2.00	1.25	1.00
Broth Only	-	-	-	-	-	-
Broth and Samples	+	+	+	+	+	+

	Gram Positive		*Gram Negative*		*Fungi*	
	S. aur	***B. sub***	***E. coli***	***P. aer***	***C. alb***	***T. rub***
$Cipro_{MIC}$ (μg/mL)	5.00	5.00	10.00	>10.00	ND	ND
$Cipro_{MMC}$ (μg/mL)	5.00	10.00	10.00	>10.00	ND	ND
Ket_{MIC}	ND	ND	ND	ND	0.25%	1.00%
Ket_{MMC}	ND	ND	ND	ND	5.00%	1.00%

Conc. = Concentration; *S. aur = Staphylococcus aureus*; *B. sub = Bacillus subtilis*; *E. coli = Escherichia coli*; *P. aer = Pseudomonas aeruginosa*; *C. alb = Candida albicans*; *T. rub = Trichophyton rubrum*; *Cipro = Ciprofloxacin*; *Ket = Ketoconazole*; (-) *Means NO GROWTH*; (+) *Means GROWTH*; *ND = Not determined*

Molecular Docking

The 3D representation of the selected protein receptors is presented in Fig. 5. The active SiteMap analysis of the receptors (Tables 3 – 5) revealed the best values (in terms of SiteScore and DScore) as Site 1 for the bacteria species *E. coli* (Table 3) and *S. aur* (Table 4), and Site 2 for the fungi species *C. alb* (Table 5).

The molecular docking results of the compounds are ranked according to their molecular docking scores (Fatriansyah *et al*., 2025), as presented in Tables 6 – 8. Site 1 gave the lowest docking scores for the *E. coli* and *C. alb* receptors, while site 2 gave the lowest scores for the *S. aur* receptor. Amongst the complexes, the heteroleptic nickel complex, 6, gave the best docking scores against the receptors used (-5.667 kcal/mol for *E. coli*, -6.614 kcal/mol for *S. aur* and -5.542 kcal/mol for *C. alb*) – poses were not obtained for all other heteroleptic complex. The high negative value (for 6) suggests good stability and interaction with the receptors (Abiodun *et al*., 2025). The homoleptic zinc complex, 4, gave better docking scores than other members of its series. Although a slightly lower docking score is observed for 6 at site 1 of the *S. aur* receptor (Table 9), a significantly better interaction is observed for other complexes; a similar effect is observed at site 2 of the *C. alb* receptor (Table 10). In the case of *E. coli* and *S. aur* receptors, the control (Ciprofloxacin) displayed less favourable scores than 6, 4 and ascorbic acid (HA_2) {Tables 6 and 7), while ketoconazole (the control in the case of *C. alb*) displayed more favourable scores than the ligands and complexes (Table 8).

Hydrogen bonding interactions dominates the protein-ligand interactions of the receptors studied (Tables 6 – 8 and Figs. 6 – 8), although π-interactions (π-cation/π-π stacking) as well as salt bridges are also involved in the interactions of the ligands/complexes with the receptors.

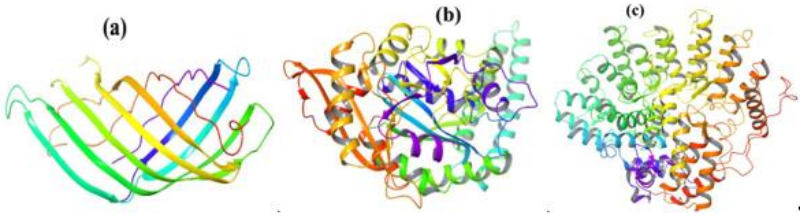

Figure 5: 3D structures of (a) *Escherichia coli (E. coli*), (b) *Staphylococcus aureus* (*S. aur*) and (c) *Candida albicans* (*C. alb*) receptors deployed

Table 3: Active SiteMap Analysis of *Escherichia coli* (*E. coli* – 1BXW)

	SiteScore	**DScore**	**Volume**	**Phobic**	**Philic**	**Residue**
***E. coli* (1BXW)**						
Site 1	1.008	1.029	783.755	0.556	1.021	Chain A: 12, 14, 19, 20, 21, 21B, 22, 23, 24, 26, 27, 28, 29, 30, 31, 32, 33, 37, 56, 57, 58, 60, 61, 62, 63, 64, 64A, 67, 68, 68A, 69, 70, 71, 72, 74, 75, 76, 100, 102, 104, 106, 107, 108, 109, 110, 116, 117, 118, 119, 120, 122, 142, 143, 144, 146, 148, 149, 150, 151, 156, 157A, 158, 160, 161
Site 3	0.789	0.851	47.677	3.660	0.024	Chain A: 7, 9, 41, 42, 43, 51, 52, 53, 79, 172
Site 2	0.638	0.521	89.866	0.088	1.235	Chain A: -1 ,0, 1, 2, 3, 4, 6, 47, 133, 134, 168, 169, 170, 171, 171A

Table 4: Active SiteMap Analysis of *Staphylococcus Aureus* (*S. aur* – 6SNR)

	SiteScore	**DScore**	**Volume**	**Phobic**	**Philic**	**Residue**
***S. aur* (6SNR)**						
Site 1	1.019	1.042	1030.37	0.630	1.005	Chain A: 19, 20, 22, 23, 24, 29, 32, 33, 36, 38, 58, 71, 73, 74, 79, 80, 81, 110, 111, 112, 115, 116, 117, 118, 119, 142, 143, 144, 147, 149, 167, 196, 199, 200, 202, 203, 205, 206, 207, 208, 212, 213, 215, 216, 304, 315, 316, 317, 318, 319, 320, 321, 322, 323, 324, 325, 326, 328,

	SiteScore	DScore	Volume	Phobic	Philic	Residue
***S. aur* (6SNR)**						
						331, 332, 333, 334, 336, 337, 351, 353, 354, 355, 356, 370, 373, 374, 376, 377, 380, 382, 384
Site 2	0.851	0.879	222.26	0.396	0.726	Chain A: 38, 60 ,61, 62, 63, 69, 103, 106, 131, 137, 138, 139, 140, 141, 142, 143, 144, 398, 400, 401, 402
Site 3	0.746	0.733	156.41	0.407	0.898	Chain A: 3, 4, 5, 6, 8, 27, 28, 30, 31, 34, 39, 40, 41, 42, 43, 44, 92, 96
Site 4	0.500	0.465	34.99	0.288	0.606	Chain A: 67, 98, 101, 102, 392, 393

Table 5: Active SiteMap Analysis of *Candida Albicans* (*C. alb* – 3DRA) Receptor

	SiteScore	DScore	Volume	Phobic	Philic	Residue
***C. alb*. (3DRA)**						
Site 2	1.082	1.026	299	0.552	1.247	Chain A: 218, 220, 223, 224, 227, 228, 231, 235, 236, 237, 258, 259, 262, 263, 265, 266, 269, 270, 281, 288, 289, 292, 295, 296, 298, 299, 302, 303; Chain B: 206, 207, 237, 238, 240, 241, 242, 244, 245, 246, 248, 249, 250, 251, 252, 253, 254, 255, 258, 259, 276, 277, 286, 289, 290, 291, 308, 312
Site 1	1.054	1.023	603	0.546	1.178	Chain A: 61, 62, 63, 64, 65, 66, 67, 71, 74, 75, 78, 97, 99, 100, 101, 102, 103, 104, 106, 107, 110, 111, 136, 139, 140, 143, 144, 145, 148, 149, 151, 152, 155, 160, 180, 183, 184, 187, 188, 192, 193, 221, 224, 225, 227, 228, 232; Chain B: 15, 16, 19, 20, 21, 23, 24, 25, 26, 27, 29, 30, 31, 32, 33, 34, 37, 78, 88, 89, 93, 94, 95, 96, 99, 129, 130, 133, 134, 139, 140, 143, 144, 145, 146, 147, 152, 153, 154, 155, 156, 157, 158, 160, 161, 164, 202, 203, 204, 205, 206, 207, 212, 213, 214, 215, 216, 217, 218, 222, 289, 300, 344, 345, 346, 347, 348, 352, 1721, 3198, 3339, 5175, 5192, 5236
Site 3	0.784	0.764	63	0.276	1.052	Chain A: 178, 217, 218, 256; Chain B: 254, 255, 256, 258, 259, 260, 260A, 272, 273, 274, 277, 278, 279, 282
Site 4	0.703	0.674	40	0.444	0.884	Chain A: 17, 18, 19, 20, 21, 22, 23; Chain B: 57, 58, 60, 61, 65, 84
Site 5	0.625	0.572	37	0.108	1.043	Chain B: 43, 46, 48, 50, 55, 105, 106, 108, 368, 379, 380, 383

Table 6: Docking Scores and Protein-Ligand Interactions of the Compounds with *Escherichia Coli* Receptor

Receptor (protein)	Compound	Docking Score (kcal/mol)	Type of Interaction	Amino acid residue	Distance (Å)
E. coli (1BXW) Site 1	6	-5.667	π-π stacking	TRP 102	3.71; 4.05; 4.08
			H-bond	ASP 20	2.04
				THR 21	2.05
				ASN 146	2.41
				TYR 72	2.71
	HA_2	-5.629	H-bond	HIS 19	1.78
				ASP 158	1.79
				TYR 72	2.12
	4	-4.670	π-π stacking	TYP 120	3.66; 4.03; 4.05
			H-bond	ASN 146	2.23
				ASP 20	2.70
	2	-4.211	π-π stacking	TRP 102	3.76; 3.89; 4.00
			H-bond	ASN 146	2.00
	3	-4.059	π-π stacking	TRP 102	3.71; 3.90; 4.01
			H-bond	ASN 146	1.95
	HA_1	-3.873	π-π stacking	HIS 19	5.02
			H-bond	ASP 56	2.00
				GLN 142	2.10

Receptor (protein)	Compound	Docking Score (kcal/mol)	Type of Interaction	Amino acid residue	Distance (Å)
				ASP 158	2.26
	Cipro	-5.379	π-cation	TRP 102	4.67
			H-bond	ASP 158	1.66
			Salt bridge	ASP 158	2.66

Cipro = Ciprofloxacin

Table 7: Docking Scores and Protein-Ligand Interactions of the Compounds with *Staphylococcus Aureus* Receptor

Receptor (protein)	Compound	Docking Score (kcal/mol)	Type of Interaction	Amino acid residue	Distance (Å)
S. aur (6SNR) Site 2	6	-6.614	π-cation	LYS 60	5.40
			H-bond	LYS 139	1.79; 1.96
	4	-4.751	H-bond	ILE 400	2.66
	HA_2	-4.468	H-bond	GLU 387	1.68
				LYS 139	2.01
				LYS 131	2.25
	2	-3.829	H-bond	ILE 400	1.92
	3	-3.603			
	HA_1	-3.160	H-bond	ILE 400	2.20
	Cipro	-4.183	H-bond	GLU 401	1.69
				TRP 38	2.15
			Salt bridge	LYS 60	2.64
				GLU 401	4.75

Cipro = Ciprofloxacin

Table 8: Docking Scores and Protein-Ligand Interactions of the Compounds with *Candida Albicans* Receptor

Receptor (protein)	Compound	Docking Score (kcal/mol)	Type of Interaction	Amino acid residue	Distance (Å)
C. alb (3DRA) Site 1	HA_2	-6.912	H-bond	TYR A: 67	1.88
				TYR A: 103	1.90; 2.08; 2.12
				GLU B: 156	2.65
			Salt bridge	ARG B: 160	3.25
	6	-5.542	H-bond	SER A: 65	1.96
				ASP B: 158	2.08
				ARG B: 160	2.18
				SER B: 212	2.24
				GLN A: 140	2.36
				GLU B: 156	2.53
			Salt bridge	ARG B: 160	3.19
	4	-4.920	π-π stacking	PHE B: 99	5.47
			H-bond	TYR A: 67	2.57
	3	-4.242	H-bond	TYR A: 67	2.36
	HA_1	-3.785	π-π stacking	TYR A: 67	5.30
			H-bond	GLU B: 156	1.90; 2.02
				ASP B: 158	1.91
	2	-2.965			
	Ket	-8.288	π-π stacking	PHE B: 99	4.96
				PHE B: 222	5.39
			Halogen-bond	LEU B: 374	3.20
				TYR B: 102	3.44

Ket = Ketoconazole

Table 9: Docking Scores and Protein-Ligand Interactions of the Compounds with *Staphylococcus Aureus* Receptor

Receptor (protein)	Compound	Docking Score (kcal/mol)	Type of Interaction	Amino acid residue	Distance (Å)
S. aur (6SNR) Site 1	6	-6.153	H-bond	LYS 374	1.75
				LEU 319	2.02
	2	-5.746	π-π stacking	PHE 205	5.11
			H-bond	PHE 354	1.96
				TYR 318	2.52
				LEU 319	2.59
	3	-5.679	π-π stacking	PHE 205	4.84
			π-cation	LYS 374	5.46
			H-bond	PHE 354	2.28
				LEU 319	2.31
	4	-5.002	H-bond	GLN 143	2.37
	HA_2	-4.891	H-bond	ASP 22	1.89
				ARG 74	1.92; 2.02
				GLN 143	2.02
	HA_1	-4.102	H-bond	GLN 143	1.79
				ASP 22	1.99
				ARG 74	2.22; 2.61

Receptor (protein)	Compound	Docking Score (kcal/mol)	Type of Interaction	Amino acid residue	Distance (Å)
	Cipro	-5.905	H-bond	TYR 320	1.76
				ASP 22	1.95
			Salt bridge	ASP 22	2.90
				ASP 353	4.72

Cipro = Ciprofloxacin

Table 10: Docking Scores and Protein-Ligand Interactions of the Compounds with *Candida Albicans* Receptor

Receptor (protein)	Compound	Docking Score (kcal/mol)	Type of Interaction	Amino acid residue	Distance (Å)
C. alb (3DRA) Site 2	HA_2	-6.714	H-bond	GLU A: 262	1.84
				LYS A: 266	2.03
				ASN A: 224	2.09; 2.11
			Salt bridge	LYS A: 266	2.95
	6	-6.184	H-bond	ILE B: 206	1.71
				ASN A: 224	1.73
				GLU A: 262	1.74
				ASN B: 207	2.18
				LYS A: 266	2.63
			Salt bridge	LYS A: 266	2.79
	4	-5.745	H-bond	ASN B: 207	1.97
				GLU A: 262	2.73
	3	-4.745	H-bond	GLU A: 231	2.09
	2	-4.154	π-cation	LYS A: 266	4.41
	HA_1	-3.962	π-π stacking	HIS B: 249	4.28
			H-bond	GLU B: 289	1.69
				ASN B: 207	2.03
	Ket	-5.015	π-π stacking	HIS B: 249	3.87
			H-bond	LYS A: 266	1.87
				ASN B: 286	2.13
			Halogen bond	LYS B: 241	2.46

Ket = Ketoconazole

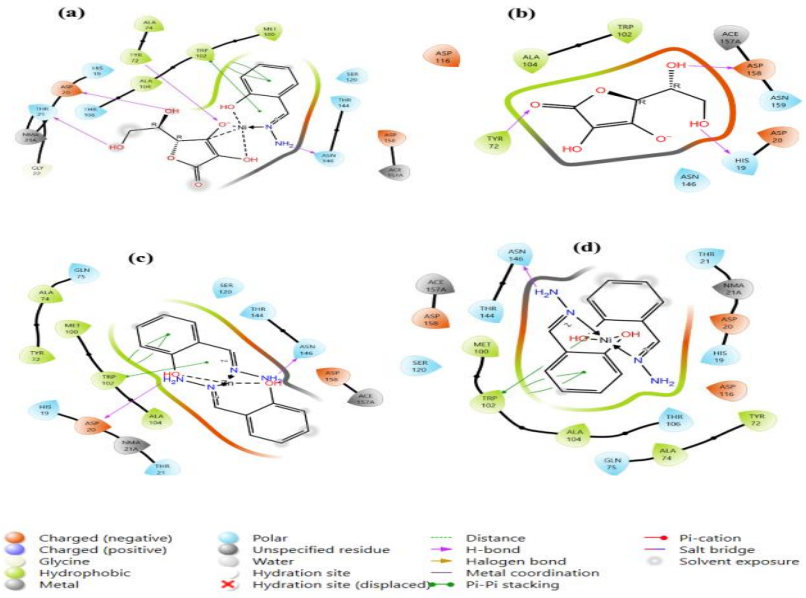

Figure 6: Protein-Ligand interaction of (a) 6 (b) HA_2 (c) 4 and (d) 2 with *Escherichia coli* receptor

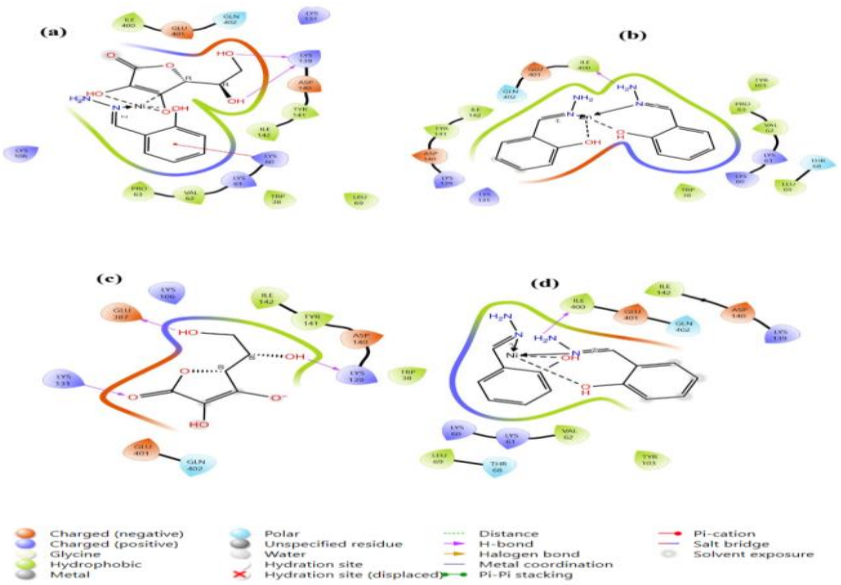

Figure 7: Protein-Ligand interaction of (a) 6 (b) 4 (c) HA_2 and (d) 2 with *Staphylococcus aureus* receptor

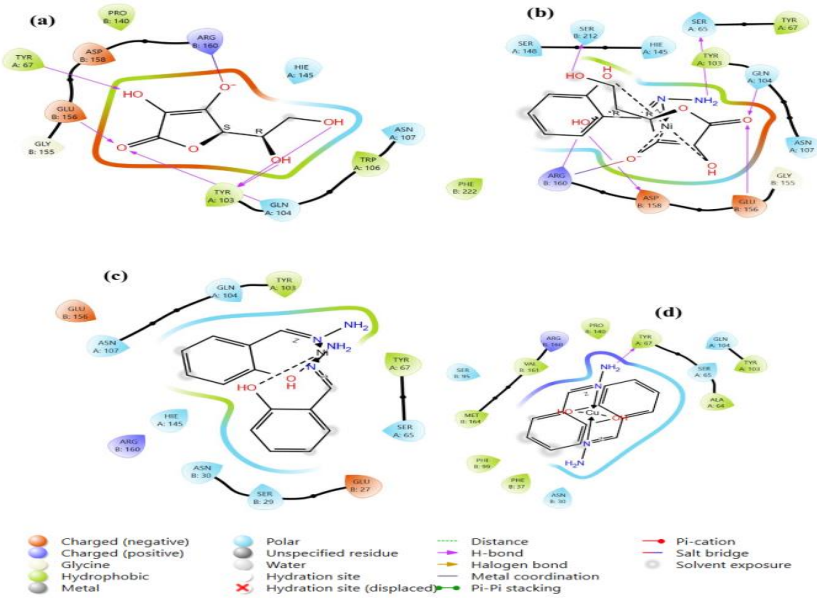

Figure 8: Protein-Ligand interaction of (a) HA_2 (b) 6 (c) 4 and (d) 3 with *Candida albicans* receptor

Frontier Molecular Orbital (FMO):

The FMO analysis was carried out to examine the relative chemical stability and reactivity of the prepared compounds. The calculated energies for the highest occupied molecular orbital (HOMO) and the lowest unoccupied molecular orbital (LUMO) are listed in Table 11, and the pictorial representation presented in Fig. 9. Electron distribution in the ligands (HA_1 and HA_2) follow essentially the same pattern, with electrons distributed over the entire molecules in the HOMO and LUMO; although, electrons in the hydroxyl (-OH) group of the HOMO move into other portions of each molecule in the LUMO. The E_{gap} values obtained suggest the ligands are more stable than the complexes, with HA_2 having the highest stability – thus charge transfer occurs from the ligands; the nucleophilic nature of the ligands is also seen from the lower electrophilicity (ω) values obtained (Table 11), in comparison to the complexes (Çınarlı *et al*., 2025) – except for the Zn complex, 4, which has a value slightly lower than that of HA_2. The homoleptic complexes have higher E_{gap} values than their respective mixed-ligand analogues. Although the E_{gap} for 1_α and 1_β are very close, those for 3_α and 3_β as well as for 7_α and 7_β are farther apart and suggest 3_α and 7_α are more stable than their respective spin-down (β) variants (3_β and 7_β) – the 3_β and 7_β variants are also the least nucleophilic (most electrophilic). The lower E_{gap} observed for 6 suggest better binding affinity (Sule *et al*., 2025) with protein receptors – possibly accounting for the higher docking scores obtained for 6 against tested receptors (Tables 6 – 8), in comparison to other complexes.

Table 11: Global Reactivity Descriptors of HA_1, HA_2 and 1 – 8 (eV)

	E_{LUMO}	E_{HOMO}	E_{gap}	I.E	E.A	η	S	χ	μ	ω
HA_1	-0.7754	-5.3658	4.5904	5.3658	0.7754	2.2952	0.4357	3.0706	-3.0706	2.0540
HA_2	-0.9018	-6.4982	5.5964	6.4982	0.9018	2.7982	0.3578	3.7000	-3.7000	2.4462
1_α	-1.7238	-5.8442	4.1204	5.8442	1.7238	2.0802	0.4807	3.7840	-3.7840	3.4417
1_β	-1.8803	-6.0562	4.1759	6.0562	1.8803	2.0880	0.4789	3.9683	-3.9683	3.7709
2	-2.0681	-5.8020	3.7339	5.8020	2.0681	1.8670	0.5356	3.9351	-3.9351	4.1470
3_α	-1.6613	-5.7919	4.1306	5.7919	1.6613	2.0653	0.4842	3.7266	-3.7266	3.3621
3_β	-3.0218	-5.7748	2.7530	5.7748	3.0218	1.3765	0.7265	4.3983	-4.3983	7.0269
4	-1.1208	-5.0236	3.9028	5.0236	1.1208	1.9514	0.5125	3.0722	-3.0722	2.4184
6	-2.5500	-5.7780	3.2280	5.7780	2.5500	1.6140	0.6196	4.1640	-4.1640	5.3714
7_α	-1.9040	-5.7136	3.8096	5.7136	1.9040	1.9048	0.5250	3.8088	-3.8088	3.8080
7_β	-3.6006	-5.6793	2.0787	5.6793	3.6006	1.0394	0.7637	4.6400	-4.6400	10.3567
8	-1.8038	-5.7472	3.9434	5.7472	1.8038	1.9717	0.5072	3.7755	-3.7755	3.6138

$E_{gap} = E_{LUMO} - E_{HOMO}$; Ionisation Energy (I.E) = - E_{HOMO}; Electron Affinity (E.A) = - E_{LUMO}; Global Hardness (η) = $\frac{I.E - E.A}{2}$; Global Softness (S) = $\frac{1}{\eta}$; Electronegativity (χ) = $\frac{I.E + E.A}{2}$; Chemical potential (μ) = - χ; Electrophilicity (ω) = $\frac{\mu^2}{2\eta}$;

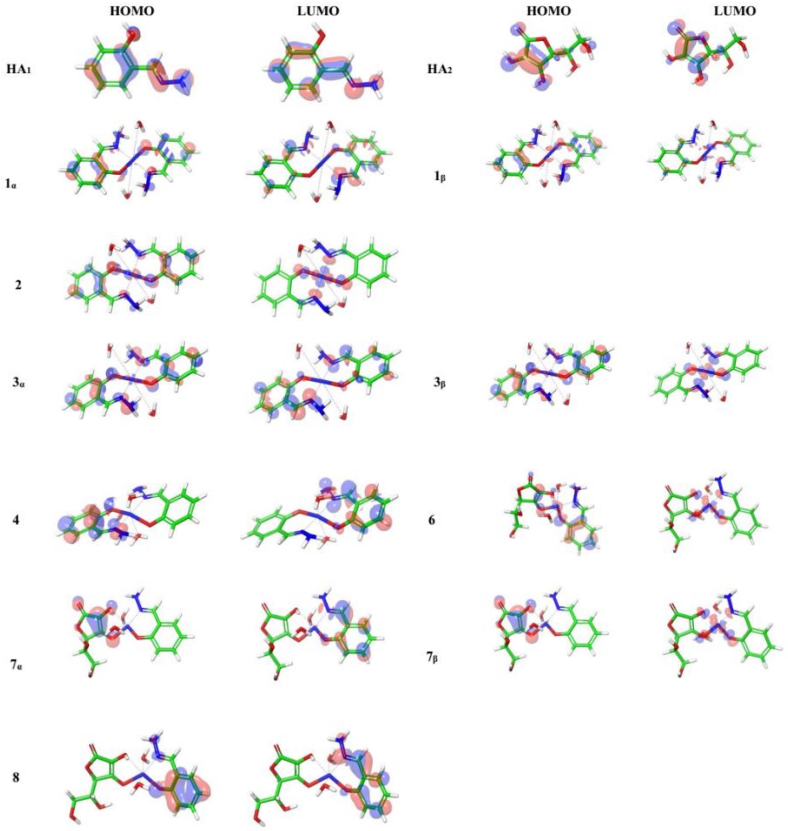

Figure 9: Frontier Molecular Orbital of the Studied Compounds

CONCLUSION

Four (4) binary Schiff bases and their respective ternary complexes with ascorbic acid were prepared and characterised. The ligands displayed π → π* and n → π* transitions, the π → π* transition undergoes a blue shift in the binary complexes and a slight red shift in the mixed ligand complexes. Infrared (IR) measurements suggest involvement of the imine (C=N) and OH groups upon metal coordination. The Co(II) complexes displayed significantly higher magnetic moment than expected for octahedral geometry and indicate orbital contribution from the $^4T_{1g}$ ground state; the Ni(II) complexes also showed a similar trend and indicate incomplete quenching of the $^3A_{2g}$ ground state; the observed subnormal value for the Cu(II) complex, **3**, indicate copper-copper interactions or antiferromagnetic property. An octahedral geometry is proposed for all the complexes. Antimicrobial evaluation suggests broad spectrum activity for the prepared compounds against tested organisms and the introduction of ascorbic acid (in the mixed ligand complexes) appears to be favourable in observed biological activity.

REFERENCES

Abdelrhman, E. M., El-Shetary, B. A., Shebl, M. & Adly, O. M. I. (2021). Coordinating behavior of hydrazone ligand bearing chromone moiety towards Cu(II) ions: Synthesis, spectral, density functional theory (DFT) calculations, antitumor, and docking studies. *Applied Organometallic Chemistry*, 35:e6183 https://doi.org/10.1002/aoc.6183

Abiodun R. O., Ogwuche S., Eugene-Osoikhia. T. 2025 "Synthesis, Characterization, and In Silico Studies of Tricarbonyl[H⁴-5-(N-(4-hydroxyphenyl)cinnamamide)cyclohexa-1,3-diene] iron and Its Demetallated Derivative as Potential Antileishmanial Agents" *FUDMA Journal of Science*, 9(11), 356 – 366 https://doi.org/10.33003/fjs-2025-0911-3670

Antimicrobial Resistance Collaborators. (2022). Global burden of bacterial antimicrobial resistance in 2019: a systematic analysis" *The Lancet*, 399(10325), 629 – 655. https://doi.org/10.1016/S0140-6736(21)02724-0

Çınarlı, M., Ataol, Ç. Y., Zeyrek, C. T., Öğütcü, H., Açık, L. & Batı, H. (2025). Design, synthesis, characterization, theoretical calculations, molecular docking studies, and biological evaluation of new Fe(II) and Cu(II) complexes of 2-acetylpyridine derivative sulfonyl hydrazone Schiff base. *Journal of Molecular Structure*, 1321, 140112 https://doi.org/10.1016/j.molstruc.2024.140112

Demirbağ, B., Yıldırım, M., Çimentepe, M., Necip, A., Ünver, H. & Tiftik, E. N. (2025). Salicylaldehyde-derived Hydrazones: Synthesis, characterization, antibacterial activity, antioxidant and anti-inflammatory effects on LPS-induced RAW264.7 macrophage cells, drug-likeness properties, and molecular docking analysis. *Biochemical and Biophysical Research Communications*, 766, 151872 https://doi.org/10.1016/j.bbrc.2025.151872

Dey, A., Roy, S. & Das, S. (2025). Recent advances in five-coordinate Co(II) single ion magnets. *Crystal Engineering Communication*, 27, 7460 – 7483 http://dx.doi.org/10.1039/d5ce00761e

Duffey, M., Shafer, R. W., Timm, J., Burrows, J. N., Fotouhi, N., Cockett, M. & Leroy, D. (2024). Combating antimicrobial resistance in malaria, HIV and tuberculosis. *Nature Reviews Drug Discovery*, 23, 461 – 479 https://doi.org/10.1038/s41573-024-00933-4

El-Asmy, A. A. & Al-Hazmi, G. A. A. (2009). Synthesis and spectral feature of benzophenone-substituted thiosemicarbazones and their Ni(II) and Cu(II) complexes. *Spectrochimica Acta Part A: Molecular and Biomolecular Spectroscopy*, 71, 1885 – 1890 http://dx.doi.org/10.1016/j.saa.2008.07.005

El-Gammal, O. A., Abdel-Latif, E., Farag, M. G. & Abdel-Rhman, M. H. (2021). Synthesis, characterization, and anticancer activity of new binuclear complexes of 2,2′-malonylbis(*N*-phenylhydrazine-1-carbothioamide). *Applied Organometallic Chemistry*, 35(5): e6194 https://doi.org/10.1002/aoc.6194

El-Sherbini, S. S., El-Reash, G. M. A. & El-Gamil, M. M. (2026). Multifunctional Schiff base cyanoacetohydrazide complexes of Manganese, Cobalt, Copper, and Zinc: Spectroscopic, DFT, fluorescence, bioactivity investigations, and molecular docking. *Inorganic Chemistry Communications*, 188, 116623 https://doi.org/10.1016/j.inoche.2026.116623

El-Sherif, A. A., Shoukry, M. M. & Abd-Elgawad, M. M. A. (2012). Synthesis, characterization, biological activity and equilibrium studies of metal(II) ion complexes with tridentate hydrazone ligand derived from hydralazine. *Spectrochimica Acta Part A: Molecular and Biomolecular Spectroscopy*, 98, 307 – 321 http://dx.doi.org/10.1016/j.saa.2012.08.034

Fabretti, A. C., Franchini, G. C. & Peyronel, G. (1982). Cobalt(II), Nickel(II), Copper(II) and Copper(I) Complexes of 2-Mercapto-5-methyl-l,3,4-thiadiazole and 2,5-Bis(methylmercapto)-1,3,4-thiadiazole. *Transition Metal Chemistry*, 7, 105 – 108 http://dx.doi.org/10.1007/BF00618193

Fatriansyah, J. F., Pradana, A. F., Driasaditya, A., Sinaga, A. A., Sahlan, M. & Surip, S. N. (2025). Molecular Docking and Molecular Dynamics Study of Propolis Compounds of Sulabiroin-A, Sulabiroin-B, and Broussoflavonol F Toward Tuberculosis 3PTY Target Protein. *Journal of Tropical Medicine* Volume 2025, Article ID 6631193, 13 pages https://doi.org/10.1155/jotm/6631193

Gęgotek, A. & Skrzydlewska, E. (2022). Antioxidative and Anti-Inflammatory Activity of Ascorbic Acid. *Antioxidants*, 11, 1993; 18 pages. https://doi.org/10.3390/antiox11101993

Gupta, N., Kaur, T., Bhalla, V., Parihar, R. D., Ohri, P., Kaur, G. & Kumar, M. (2017). A naphthalimide-based solid state luminescent probe for ratiometric detection of aluminum ions: *in vitro* and *in vivo* applications. *Chemical Commununications*, 53, 12646 – 12649 http://dx.doi.org/10.1039/c7cc07996f

Hast, M. A. & Beese, L. S. (2008). Structure of Protein Geranylgeranyltransferase-I from the Human Pathogen *Candida albicans* Complexed with a Lipid Substrate. *Journal of Biological Chemistry*, 283(46), 31933 – 31940 https://doi.org/10.1074/jbc.M805330200

Hollis, L. S., Stern, E. W., Amundsen, A. R., Miller, A. V. & Doran, S. L. (1987). Platinum Complexes of Vitamin C. NMR Studies on the Solution Chemistry of m-Pt(diamine)(ascorbate) Complexes. *Journal of the American Chemical Society*, 109, 3596 – 3602 https://doi.org/10.1021/ja00246a016

Ieque, A. L., Palomo, C. T., Spanhol, V. G. de F., Dacome, M. L. F. da M., Pereira, J. J. do C., Candido, F. C., Caleffi-Ferracioli, K. R., Siqueira, V. L. D., Cardoso, R. F., Vandresen, F., Alves-Olher, V. G. & Scodro, R. B. de L. (2024). Preclinical tests for salicylhydrazones derivatives to explore their potential for new antituberculosis agents. *Tuberculosis*, 148, 102545 https://doi.org/10.1016/j.tube.2024.102545

Jaguar, version 11.9, Schrodinger, Inc., New York, NY, 2023.

Jha, N. N & Ray, I. P (2000). Magnetic Studies on Ni(II) and Co(II) Complexes of Hydroxamic Acid. *Asian Journal of Chemistry*, 12(3), 703 – 706

Kaushik, A., Peshrana, A., Barapatre, R., Pansheriya, S. & Kaushal, R. S. (2025). Unveiling the properties of ascorbic acid against *M. tb* through in silico approach: A comparative drug-based study. *Journal of Molecular Modeling*, 31:94, 24 pages https://doi.org/10.1007/s00894-025-06322-x

Lu, X., Nan, M., Zhang, H., Liu, X., Yuan, H. & Yang, J. (2007). Investigation of the Antioxidant Property of Ascorbic Acid. *The Journal of Physical Chemistry C*, 111, 14998 – 15002 https://doi.org/10.1021/jp072551i

Malviy, K., Shrivastava, S. & Sonwane, S. (2021). Synthesis, Characterization and Antimicrobial Activity of Mixed Ligand Complexes of Inner Transition Metal with L-Ascorbic acid, its Derivative and Adenine Base. *Journal of Advanced Scientific Research*, 12 (3) Suppl 2: 188 – 197 https://doi.org/10.55218/JASR.s2202112322

Okafor, E. C. (1978). On the Condensation of Salicylaldehyde with Hydrazine. *Talanta*, 25(4), 241 – 242 https://doi.org/10.1016/0039-9140(78)80016-2

Onyenze, U., Otuokere, I. E. & Igwe, J. C. (2016). Co(II) and Fe(II) mixed ligand complexes of Pefloxacin and Ascorbic acid: Synthesis, Characterization and Antibacterial Studies. *Research Journal of Science and Technology*, 8(4), 215 – 220 https://doi.org/10.5958/2349-2988.2016.00032.2

Pautsch, A. & Schulz, G. E. (1998). Structure of the outer membrane protein A transmembrane domain. *Nature Structural Biology*, 5(11), 1013 – 1017 https://doi.org/10.1038/2983

Rathi, M., Devi, J., Dhillayan, N., Asija, S. (2026). Bioactive Transition Metal (II) Hydrazone Complexes: Spectral Elucidation, Antimalarial, Antioxidant, and Antimicrobial Activities Correlated With Molecular Docking and Absorption, Distribution, Metabolism, Excretion, and Toxicity. *ChemMedChem*. 21:e202501071 https://doi.org/10.1002/cmdc.202501071

Ribeiro, N. & Correia, I. (2024). A review of hydrazide-hydrazone metal complexes' antitumor potential. *Frontiers in Chemical Biology*, 3, 1398873https://doi.org/10.3389/fchbi.2024.1398873

Rupa, S. A., Moni, M. R., Patwary, M. A. M., Mahmud, M. M., Haque, M. A., Uddin, J. & Abedin, S. M. T. (2022). Synthesis of Novel Tritopic Hydrazone Ligands: Spectroscopy, Biological Activity, DFT, and Molecular Docking Studies. *Molecules*, 27, 1656, 20 pageshttps://doi.org/10.3390/molecules27051656

Sogukomerogullari, H. G., Başaran, E., Çakmak, R., Muhammed, M. T. & Akkoc, S. (2025). Novel transition metal (II) complexes of hydrazones as potential antitumor agents: Synthesis, characterization, DFT computations, cytotoxic activities, molecular docking and simulation studies. *Inorganic Chimica Acta*, 581, 122634 https://doi.org/10.1016/j.ica.2025.122634

Sule, A. O., Obiyenwa, K. G., Salawu, O. W. & Banjo S. (2025). In silico evaluation of Co(II), Mn(II), Cu(II), and Zn(II) complexes with hydrazide ligands: DFT, spectroscopic, and molecular docking studies. *International Journal of Chemical Studies*, 13(3), 96 – 113https://www.doi.org/10.22271/chemi.2025.v13.i3b.12545

Tafere, D. A., Gebrezgiabher, M., Elemo, F., Sani, T., Atisme, T. B., Ashebr, T. G. & Ahmed, I. N. (2025). Hydrazones, hydrazones-based coinage metal complexes, and their biological applications. *RSC Advances*, 15, 6191 – 6207 https://doi.org/10.1039/d4ra07794f

Wadday, F. Y. & Hussein, A. A. (2022). Synthesis, Identification, Thermodynamic and Biological Studies of New Ligand Derivative from L-ascorbic acid and its Complexes with some Metal ions. *Research Journal of Pharmacy and Technology*, 15(8), 3452 – 3458https://doi.org/10.52711/0974-360X.2022.00578

York, A., Lloyd, A. J., del Genio, C. I. Shearer, J., Hinxman, K. J., Fritz, K., Fulop, V., Dowson, C. G., Khalid, S. & Roper, D. I. (2021). Structure-based modeling and dynamics of MurM, a Streptococcus pneumoniae penicillin resistance determinant present at the cytoplasmic membrane. *Structure*, 79, 731 – 742 https://doi.org/10.1016/j.str.2021.03.001

Yuge, H. & Miyamoto, T. K. (1996). New Synthesis and Crystal Structures of Platinum(II) L-Ascorbate Complexes. *Chemistry Letters*, 375 – 376 https://doi.org/10.1246/cl.1996.375

Yuge, H. & Miyamoto, T. K. (2002). Steric influence on platinum(II) ascorbate complexes. *Inorganica Chimica Acta*, 329, 66 – 70 https://doi.org/10.1016/S0020-1693(01)00810-6